ORIGINAL RESEARCH

Antitumor effect of hyaluronic-acid-modified chitosan nanoparticles loaded with siRNA for targeted therapy for non-small cell lung cancer

Wenhua Zhang[1,2,*]
Wenhua Xu[1,*]
Yu Lan[3]
Xuliang He[1]
Kaibin Liu[4]
Ye Liang[2]

[1]Department of Inspection, Medical Faculty, Qingdao University, Qingdao 266003, People's Republic of China; [2]Key Laboratory, Department of Urology and Andrology, Affiliated Hospital of Qingdao University, Qingdao 266003, People's Republic of China; [3]Department of Inspection, Weihai Central Hospital, Weihai 264400, People's Republic of China; [4]Department of Clinical Medicine, Second Military Medical University, Shanghai 200433, People's Republic of China

*These authors contributed equally to this work

Correspondence: Wenhua Xu
Department of Inspection, Medical Faculty of Qingdao University, Qingdao 266003, People's Republic of China
Tel +86 1 370 899 1018
Email qd.wh@163.com

Ye Liang
Key Laboratory, Department of Urology and Andrology, Affiliated Hospital of Qingdao University, Qingdao 266003, People's Republic of China
Tel +86 1 866 180 7639
Email liangye82812@163.com

Purpose: Nanoparticle (NP)-mediated targeted delivery of therapeutic genes or siRNAs to tumors has potential advantages. In this study, hyaluronic acid (HA)-modified chitosan nanoparticles (CS NPs-HA) loaded with cyanine 3 (Cy3)-labeled siRNA (sCS NPs-HA) were prepared and characterized.

Methods: Human non-small cell lung cancer (NSCLC) A549 cells expressing receptor CD44 and tumor-bearing mice were used to evaluate the cytotoxic and antitumor effects of sCS NPs-HA in vitro and in vivo.

Results: The results showed that noncytotoxic CS NPs-HA of small size (100–200 nm) effectively delivered the Cy3-labeled siRNA to A549 cells via receptor CD44 and inhibited cell proliferation by downregulating the target gene *BCL2*. In vivo experiment results revealed that sCS NPs-HA directly delivered greater amounts of Cy3-labeled siRNA to the tumor sites, resulting in the inhibition of tumor growth by downregulating *BCL2*, as compared to unmodified NPs loaded with siRNA (sCS NPs) and to naked Cy3-labeled siRNA.

Conclusion: The HA-modified NPs based on chitosan could serve as a promising carrier for siRNA delivery and targeted therapy for NSCLC expressing CD44.

Keywords: nanoparticle, siRNA, CD44, hyaluronic acid, cancer

Introduction

Lung cancer is a common cause of cancer-related deaths worldwide,[1] and the associated high mortality rate threatens many human lives. Lung cancer includes small cell lung cancer (SCLC) and non-small cell lung cancer (NSCLC),[2] wherein NSCLC accounts for 85% of all lung cancer cases.[3] NSCLC is often diagnosed at the advanced stage, which is associated with low survival rate and poor prognosis.[4] For patients with advanced or metastatic NSCLC, chemotherapy may only prolong the survival time and improve quality of life.[3,5–8] Nonetheless, chemotherapy can also cause some damage to the patient's immune system.

Targeted gene therapy has been successfully employed against malignant tumors such as breast cancer,[9] gastric cancer,[10] colorectal cancer,[11] lymphoma, gastrointestinal stromal tumors, and chronic myelogenous leukemia.[12–16] siRNA, comprising 21–23 nucleotides, has been an attractive candidate for gene therapy. siRNA contains a sequence that is complementary to a specific protein-coding mRNA and may induce site-specific cleavage, resulting in the inhibition of protein synthesis and suppression of protein expression.[17,18] In addition, the synthesis of siRNA is relatively simple without

any necessity of cell expression systems. Therefore, siRNA has important applications to tumor-targeting therapies. Poulami Majumder et al[19] invented a CDC20 siRNA liposome formulation for the treatment of cancer antiangiogenesis using the characteristics of many cancer cells overexpressing CDC20. In addition, the Poulami Majumder team has developed an in vivo siRNA delivery system based on lipid-based TIPA-NAs, enriching the in vivo delivery system of siRNA.[20] Nevertheless, clinical application of siRNAs is limited because siRNAs are highly unstable in the circulation and may be easily degraded by ribonucleases, cleared by the renal system, or phagocytosed by the mononuclear phagocyte system in the circulation; the low rate of uptake into tumor cells, poor endosomal escape after endocytosis, and off-target effects have restricted the widespread use of siRNAs.[21–23] Therefore, it is important to develop a carrier that can efficiently deliver siRNAs to tumor cells.

Chitosan (CS) and its derivatives are considered better vectors for the delivery of siRNAs, owing to the nontoxicity, low immunogenicity, good biocompatibility and biodegradability, and low production cost of CS.[9,23,24] Under mildly acidic conditions, the primary amine groups on CS bear cationic charges and may easily bind to negatively charged substances or siRNAs via electrostatic interactions to form nanoparticles (NPs) or complexes.[25] On the other hand, the use of CS as a carrier for siRNA delivery has several limitations such as low transfection efficiency, poor cell membrane penetration, and a lack of tumor targets, resulting in the low uptake of chitosan nanoparticles (CS NPs) by tumor cells.[25] To overcome these shortcomings, CS has been modified with several chemical groups or biological materials[26–28] to enhance the efficiency of siRNA delivery.

CD44 is a complex transmembrane glycoprotein that was initially identified as a receptor for hyaluronic acid (HA) as well as a homing receptor for human cells.[29] It is a cell surface HA-binding glycoprotein that is involved in physiological and pathological processes, including wound healing, lymphocyte homing, cell migration and proliferation, and cancer invasion and metastasis.[30,31] In comparison with normal cells, many types of cancer cells such as lung, breast, pancreatic, gastric, and colon cancer cells are known to overexpress CD44, indicating its role as a potential therapeutic target in cancer.[32] HA is a linear glycosaminoglycan composed of alternating repeats of N-acetylglucosamine and glucuronic disaccharide and constitutes a major component of the extracellular matrix.[33] CD44 is a transmembrane glycoprotein and surface receptor for

HA and is involved in the cellular response to a microenvironment. HA binds to the cell surface receptor CD44 and performs a function in the regulation of signal transduction and cellular physiological functions.[34] NSCLC cell line A549 is known to overexpress CD44.[35] The use of HA-modified CS NPs (CS NPs-HA) vectors to deliver anticancer drugs as a targeted therapy for NSCLC has been reported in the literature.[31] Nonetheless, there have been no HA-modified CS NPs as siRNA (sCS NPs-HA) delivery vectors for targeted therapy for NSCLC. To further explore the antitumor effectiveness of gene delivery carriers prepared from CS and HA, we designed HA-modified CS NPs for siRNA loading. B-cell lymphoma/leukaemia 2 (Bcl2) is one of the most important oncogenes involved in cell apoptosis.[36] *Bcl2* gene can inhibit apoptosis and cell death caused by various cytotoxic factors. Therefore, we chose *Bcl2* as a targeting gene to assess the ability of sCS NPs-HA to silence the targeted gene *Bcl2* and anti-tumor effects.

In this study, CS NPs were prepared and chemically modified with HA, the resulting NPs were designated as CS NPs-HA. We explored the characteristics of CS NPs, including their particle size, zeta potential, polydispersity index (PDI), morphology, efficiency of encapsulation of cyanine 3 (Cy3)-labeled siRNA, and cytotoxicity. A549 cells expressing CD44 were chosen to study the cellular uptake and distribution of sCS NPs-HA and to evaluate the effects of these particles on the proliferation of tumor cells and the ability to silence the targeted gene *Bcl2*. Furthermore, in vivo experiments were conducted to investigate the targeting and inhibitory abilities of sCS NPs-HA against NSCLC.

Materials and methods
Materials and reagents
CS was acquired from Sigma-Aldrich (St. Louis, MO, USA). The degree of deacetylation of this CS is 92%, and the molecular weight is 35 kD. HA was purchased from Shandong Focuschem Biotech Co., Ltd., whereas sodium tripolyphosphate (TPP) and MTT were purchased from Sigma-Aldrich. Materials for cell culture, including the Roswell the Park Memorial Institute (RPMI) 1640 medium, DMEM, FBS, trypsin, penicillin, and streptomycin were supplied by Gibco (Grand Island, NY, USA). All other chemicals and reagents used in the study were of reagent grade. Cy3-labeled siRNA against *BCL2* was bought from Genepharma (Shanghai, China).

Mouse fibroblast cell line L929 and human NSCLC cell line A549 were purchased from the Typical Culture Preservation Commission Cell Bank, Chinese Academy Of Science (GNM28, TCHu150) (Shanghai, China). Female BALB/c mice (4–5 weeks old) were purchased from the Beijing Charles River Laboratory Animal Technology (Beijing, China). For the animal experiments, protocols were approved by the Institutional Animal Care and Use Committee of Affiliated Hospital of Qingdao University, and procedures were performed in accordance with the ARVO Statement for the Use of Animals (No. AHQU20170812A).

Preparation of various NPs

In brief, CS was dissolved in a 0.5% acetic acid solution, and pH was adjusted to 4–5. We employed CS and TPP to produce CS NPs by the method of ion gelation, as previously described.[37,38] Strong electrostatic interaction is reported to occur between the anionic carboxyl group of HA and the cationic amino group of CS.[27] HA was conjugated onto the surface of CS NPs by charge adsorption to obtain CS NPs-HA. We mixed Cy3-labeled siRNA targeting *BCL2* and TPP in advance and then slowly added this mixture to the CS solution during ultrasonication at 4°C to obtain CS NPs loaded with Cy3-labeled siRNA (sCS NPs) and sCS NPs-HA. CS NPs were placed in a dialysis bag for overnight dialysis to remove any free particles. We used Zetasizer Nano ZS Analyzer (DKSH-MT-CZGC-017 Nanotrac Wave, USA) and scanning electron microscopy (SEM; VEGA3, Tescan, Brno, Czech Republic) to study the physical characteristics, including particle size, zeta potential, PDI, and morphology.

Determination of siRNA-loading efficiency

We used 2 mL of CS NPs or CS NPs-HA to load 66 μg (2 optical density [OD] units) of Cy3-labeled siRNA to obtain sCS NPs and sCS NPs-HA, respectively. The efficiency of encapsulation (%) of Cy3-labeled siRNA in CS NPs and CS NPs-HA was measured by UV spectrophotometry (QuickDrop Spectrophotometer, USA). We investigated OD of the free Cy3-labeled siRNA in the supernatant of the CS NP solution at 260 nm wavelength after centrifugation (13,000 rpm, 30 mins). In addition, we measured the OD of the supernatant of CS NPs and CS NPs-HA as blank controls. Naked Cy3-labeled siRNA served as a positive control. We evaluated the efficiency of encapsulation of Cy3-labeled siRNA inside CS NPs and

CS NPs-HA as follows: encapsulation efficiency = (1 − [OD of siRNA in supernatant/OD of siRNA in initial feeding solution]) ×100%. In addition, we performed agarose gel electrophoresis to assess the encapsulation efficiency of Cy3-labeled siRNA in various CS NP preparations.

In vitro stability evaluation

To evaluate the stability of CS NPs in vitro, we incubated CS NPs, sCS NPs, CS NPs-HA, and sCS NPs-HA at room temperature. An aliquot from each solution was analyzed daily for particle size, zeta potential, and PDI for 6 consecutive days. The experiments were carried out in triplicate.

Cytotoxicity

To evaluate the cytotoxicity of CS NPs with or without the modification, we followed the international evaluation standard of cytotoxicity (GB/T16886.5-2003). The effect of CS NPs on the relative growth rate (RGR; %) of L929 cells was measured by the MTT assay. L929 cells (200 μL/well at a density of 2×10^4 cells/mL) were cultivated in a 96-well culture plate. After culturing for 24 hrs at 37°C and 5% CO_2, the cells were incubated with the medium supplemented with CS NPs or CS NPs-HA (5 μg, 10 μg, 20 μg, 40 μg, 80 μg); the control group was cultured in a fresh DMEM medium. All L929 cell groups were cultured for 24, 48, and 96 hrs. Each sample was evaluated in triplicate. After the incubation, 20 μL of the MTT solution was added into each well, and the plate was incubated for 4 hrs at 37 °C. The reaction was terminated with the addition of 200 μL of dimethyl sulfoxide into each well, followed by gentle mixing on an orbital shaker for 30 mins at room temperature. The RGR of cells was determined by measuring the absorbance at 490 nm (OD_{490}). RGR (%) was evaluated with the following formula: RGR (%) = [(OD_1 − OD_0)/(OD_2 − OD_0)] ×100%, where OD_0, OD_1, and OD_2 represent the average OD of the blank, experimental, and control groups, respectively. The results were scored according to the following criteria: 0 (RGR ≥100% means noncytotoxic), 1 (RGR ranging from 75% to 99% means slightly cytotoxic), 2 (RGR ranging from 50% to 74% means moderately cytotoxic), and 3 (RGR ranging from 25% to 49% means severely cytotoxic). All experiments were performed in triplicate.

A proliferation assay for A549 cells

We evaluated the effects of different concentrations of various Cy3-labeled siRNA-loaded[CS NPs on the proliferation of A549 cells by the MTT assay. Test groups

included cells treated with the medium supplemented with naked Cy3-labeled siRNA, sCS NPs, sCS NPs-HA, Cy3-labeled siRNA transfection, or the fresh RPMI 1640 medium alone, the cells cultured in the RPMI 1640 medium were the control group, and the experimental groups were treated with equal amounts of Cy3-labeled siRNA (0.26, 0.52, or 0.78 µg), respectively. A549 cells (200 µL/well at a density of 2×10^4 cells/mL) were cultured in a 96-well plate. After 24 hrs, A549 cells were treated with the reagents being tested. The MTT assay was conducted to evaluate the proliferation of A549 cells at 24 and 48 hrs. Each sample was analyzed in triplicate and all experiments were performed in triplicate.

Evaluation of the transfection rate

We performed a flow cytometry (FACA, Calibur, BD, USA) analysis to evaluate the transfection rate of sCS NPs and sCS NPs-HA in A549 cells. A549 cells were seeded at a density of 1.5×10^5 cells/well in a six-well plate and incubated at 37°C. Test groups included sCS NPs, sCS NPs-HA, and the Cy3-labeled siRNA transfection, and the cells cultured in the RPMI 1640 medium were the control group. After 24 hrs, the medium was replaced with that containing sCS NPs, sCS NPs-HA, or the Cy3-labeled siRNA transfection, and control group medium was replaced with fresh RPMI 1640 medium. All experimental groups were incubated with equal amounts of Cy3-labeled siRNA (2.6 µg). Then, the cells were collected at 24 and 48 hrs, respectively, for flow cytometry to detect the transfection rate.

An immunofluorescent assay

Changes in the expression of recep tor CD44 were evaluated by an immunofluorescent assay and confocal laser scanning microscopy (Leica SPE, Germany). Experimental groups included sCS NPs-HA (amounts of Cy3-labeled siRNA was 0.52 µg), and the cells cultured in the RPMI 1640 medium were the control group. A549 cells were cultured on glass slides in 24-well plates for 24 hrs, followed by their incubation with the medium with or without sCS NPs-HA. Samples were collected at 4, 8, 16, 24, and 48 hrs and fixed in 4% paraformaldehyde for 15 min, followed by their permeabilization with 0.1% Triton X-100 for 10 min and blocking with 5% BSA for 30 mins. The slides were incubated overnight with a mouse polyclonal anti-CD44 antibody (CST, Beverly, MA, USA) at 4°C, followed by treatment with fluorescein isothiocyanate–conjugated secondary antibodies (mouse anti-rabbit fluorescent secondary antibody) (Abcam, Cambridge, UK) for 1 hr at

room temperature. After a wash with PBS, nuclear staining was performed by the incubation of samples with DAPI (0.5 mg/mL) for 5 mins. The slides were washed once with PBS for 5 mins and sealed with an antifluorescence quencher (Solarbio, Beijing, China). The samples were examined under the confocal laser scanning microscope. At the same time, cells were collected at different time intervals and PCR experiments were performed to analyze the changes of CD44.

Analysis of target gene expression

Western blot analysis was performed to compare the expression levels of the target protein (*BCL2*) among different experimental groups. A549 cells were seeded at a density of 3×10^4 cells/well in a 24-well plate for 24-hr incubation, followed by their treatment with the medium with CS NPs, sCS NPs, CS NPs-HA, sCS NPs-HA, Cy3-labeled siRNA transfection (amount of Cy3-labeled siRNA was 0.52 µg), or the RPMI 1640 medium alone for 48 hrs, the cells cultured in the RPMI 1640 medium were the control group, and control group medium was replaced with fresh RPMI 1640 medium. The fluorescence intensity of A549 cells was examined under a fluorescence microscope (IX73; Olympus, Tokyo, Japan). Western blot analysis was performed on the collected cell lysates according to standard protocols. Cells were harvested and extracted with SDS sample buffer. The protein extract was boiled in a sample buffer containing SDS/beta-mercaptoethanol. The purified protein (30 µg) was separated by SDS-PAGE and transferred to a PVDF membrane, followed by blocking in 5% fat-free milk in PBST for 1 hr and then incubated overnight with the rabbit monoclonal anti-*BCL2* antibody (Abcam, Cambridge, UK) at 4°C. The next day, the blots were incubated with the appropriate HRP-conjugated secondary antibody (Jackson Immuno Research Laboratories, Pennsylvania, USA). A chemiluminescent substrate for horseradish peroxidase detection purchased from Millipore (Bedford, MA, USA) and the FluorChem Q imaging system (AlphaImage, San Jose, CA, USA) were employed to visualize the protein bands, and quantitative analysis of data.

Animal experiments

A549 cells were cultured in the RPMI 1640 medium supplemented with 10% of FBS and 1% of a penicillin and streptomycin solution. An in vivo ectopic xenograft tumor model was established via subcutaneous injection of 4×10^6 human A549 cells into the right armpits of female BALB/c mice. The tumor volumes were measured after 2 days and then every other day via the following formula: $V = (S^2 \times L)/2$, where S represents the smaller and L the

longer tumor diameter.[9] Mice were randomly subdivided into four groups after the tumor volume reached 60 ±10 mm^3 (mean ± SD, n≥3) as follows: PBS (blank), naked Cy3-labeled siRNA (negative control), sCS NPs, and sCS NPs-HA groups. Tested reagents were administered through tail vein injections every other day 10 times in total. The injection dose of Cy3-labeled siRNA in all experimental groups was 0.16 mg siRNA/kg, which means that the amount of Cy3-labeled siRNA contained in the sCS NPs group and the sCS NPs-HA group was also 0.16 mg siRNA/kg. All the mice were euthanized after the last dose, on the 20th day of dosing (day 35 post-tumor inoculation). The mice were weighed, and their tumors, liver, kidneys, and spleen were excised and weighed, and statistical analysis of tumor weights in mice was carried out and drew the tumor growth inhibition graph. The indices (weight ratios) of the liver, kidneys, or spleen toward the whole-body weight were calculated by means of the following formula: Relative weight = W/W_0, where W is the weight of the liver, kidneys, or spleen, and W_0 denotes the body weight of the experimental mice. Next, the changes in the liver, kidneys, and spleen indices among experimental groups were statistically analyzed. We then performed an immunofluorescent assay on tumor tissues and statistically analyzed the fluorescence intensity in the ImageJ software (NIH, Bethesda, MD, USA). In addition, Western blot analysis was performed to analyze the *BCL2* protein expression in tumor tissues.

Statistical analysis

All data are expressed as the mean ± SD of duplicate experiments. ANOVA or the two sample independent *t*-test were conducted for the statistical analysis of the data, and data with a *P*-value <0.05 were considered statistically significant (as computed by SPSS version 19.0).

Results
Characteristics of various CS NPs

CS NPs and CS NPs-HA were prepared first and were characterized in terms of particle size, zeta potential, and PDI (Table 1, Figure 1A). The morphology of CS NPs-HA was determined by SEM; these NPs were shown to be approximately spherical (Figure 1B). After that, siRNA-loaded NPs (sCS NPs and sCS NPs-HA) were prepared. The characteristics of sCS NPs and sCS NPs-HA are presented in Table 1 and Figure 1C. Table 1 indicates that the particle size of all NPs ranged from 100 to 130 nm, and all of them had a positive

Table 1 Characteristics of various types of CS NPs

Group	Particle size (nm)	Zeta potential (mV)	Polydispersity index (PDI)
CS NPs	103.63±3.66	38.50±1.53	0.87±0.03
CS NPs-HA	115.10±4.59	32.33±2.05	0.88±0.06
sCS NPs	124.97±2.71	29.57±0.31	0.80±0.20
sCS NPs-HA	127.13±1.88	31.03±1.93	0.64±0.21

Note: Data represent mean ± SD of three experiments.
Abbreviations: CS NPs, chitosan nanoparticles; CS NPs-HA, HA-modified chitosan nanoparticles; sCS NPs, chitosan nanoparticles loaded with siRNA; sCS NPs-HA, HA-modified chitosan nanoparticles loaded with siRNA.

surface charge; these parameters were suitable for cell uptake.[39] In addition, the PDI of all types of CS NPs was lower than "1", and sCS NPs-HA had the lowest PDI.

Efficiency of encapsulation of Cy3-labeled siRNA in CS NPs

We performed UV spectrophotometry to evaluate the encapsulation efficiency of 66 μg (2 OD) of Cy3-labeled siRNA in sCS NPs and sCS NPs-HA. As a result, encapsulation efficiency of 93–94% was observed for sCS NPs and sCS NPs-HA. The results of electrophoresis in 2% agarose gels showed that there was no detectable free Cy3-labeled siRNA, whereas sCS NPs and sCS NPs-HA manifested high efficiency of encapsulation of Cy3-labeled siRNA (Figure 1D).

Stability of CS NPs

We continuously measured the particle size, zeta potential, and PDI of CS NPs, sCS NPs, CS NPs-HA, and sCS NPs-HA for 6 days. As presented in Figure 1E, the particle size underwent no significant changes in all groups. Furthermore, no obvious changes were observed in the PDI and zeta potential except in sCS NPs; these data indicated that CS NPs with loaded siRNA were not stable. Nonetheless, this problem was resolved by HA modification of CS NPs.

Cytotoxicity of nonloaded NPs

Cytotoxicity experiments were performed on L929 cells cultured in the presence of CS NPs or CS NPs-HA in solution. The volume of CS NPs and CS NPs-HA solutions was between 5 and 80 μg. In comparison with the control group, the cells treated with CS NPs or CS NPs-HA showed no significant change in viability at 24 and 48 hrs (Figure 2A). At 96 hrs, the growth of L929 cells slightly slowed in the group treated with the highest dose (80 μg) of CS NPs, but the RGR was greater than 90%. Furthermore, a slight decrease in the growth rate of
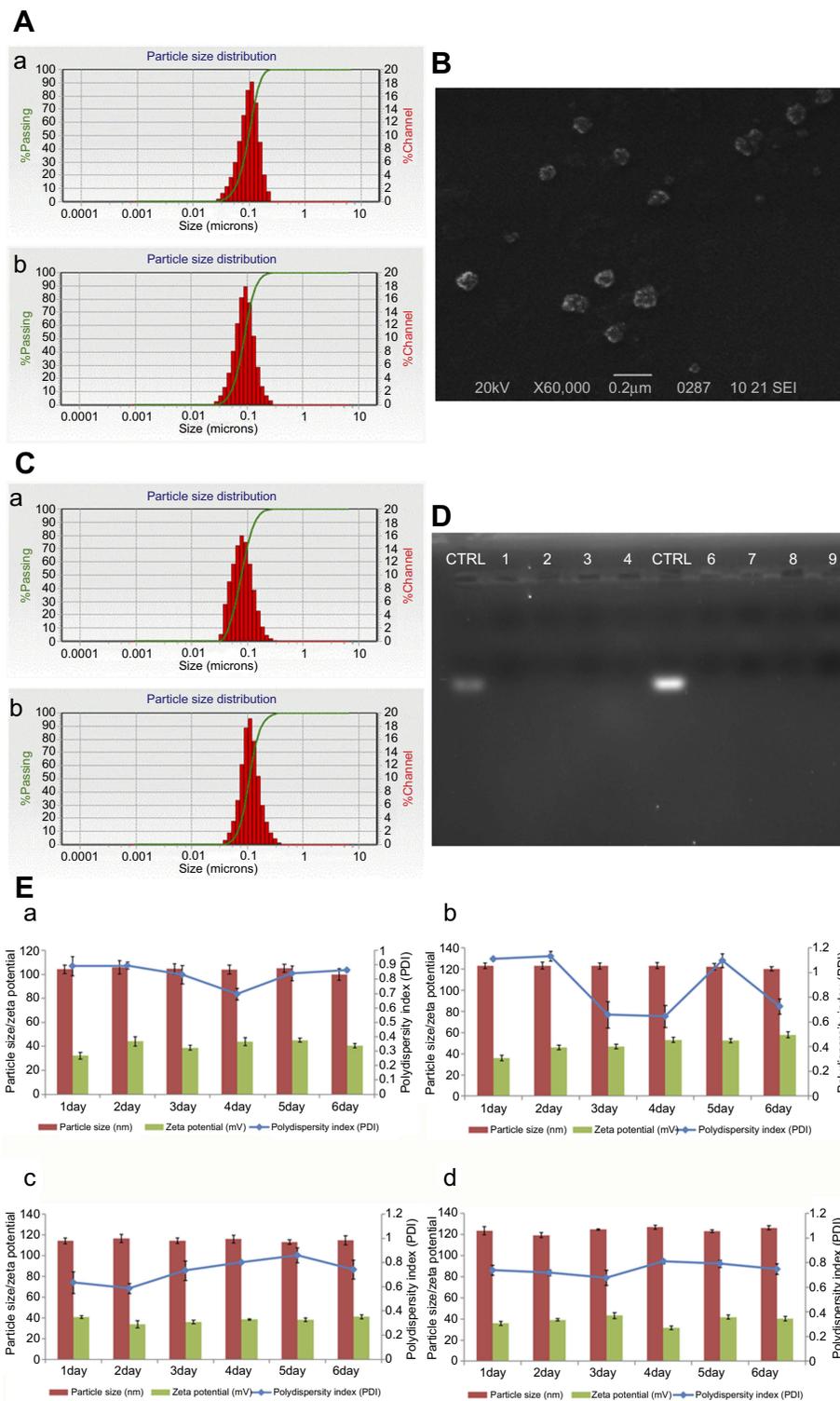
Figure 1 Characteristics of various CS NPs. (**A**) Size distributions of CS NPs and CS NPs-HA. a) CS NPs; b) CS NPs-HA. (**B**) An SEM image of CS NPs-HA. (**C**) Size distributions of sCS NPs and sCS NPs-HA. a) sCS NPs; b) sCS NPs-HA. (**D**) Cy3-labeled siRNA encapsulation efficiency of CS NPs and CS NPs-HA. A total of 0.5 μL of Cy3-labeled siRNA served as a control (CTRL); lane 1, 5.3 μL of CS NPs; lane 2, 5.3 μL of sCS NPs (containing 0.5 μL of Cy3-labeled siRNA); lane 3, 5.3 μL of CS NPs-HA; lane 4, 5.3 μL of sCS NPs-HA (containing 0.5 μL of Cy3-labeled siRNA); lane 5, 1 μL of Cy3-labeled siRNA was used as a control (CTRL); lane 6, 10.6 μL of CS NPs; lane 7, 10.6 μL of sCS NPs (containing 1 μL of Cy3-labeled siRNA); lane 8, 10.6 μL of CS NPs-HA; lane 9, 10.6 μL of sCS NPs-HA (containing 1 μL of Cy3-labeled siRNA). (**E**) In vitro stability of CS NPs. a) CS NPs; b) sCS NPs; c) CS NPs-HA; d) sCS NPs-HA (n=3).

Abbreviations: CS NPs, chitosan nanoparticles; CS NPs-HA, HA-modified chitosan nanoparticles; sCS NPs, chitosan nanoparticles loaded with siRNA; sCS NPsHA, HA-modified chitosan nanoparticles loaded with siRNA.

L929 cells was observed during treatment with the highest dose (80 μg) of CS NPs-HA, but the RGR was 89.52%. The cytotoxicity was found to be grade 1. These results suggested that the cytotoxicity of CS NPs and CS NPs-HA meets the application standards of biomedical materials, which could be used as biocompatible materials.

Proliferation of A549 cells treated with sCS NPs

In a comparison among sCS NPs group, Cy3-labeled siRNA transfection group, and naked Cy3-labeled siRNA group, sCS NPs-HA group showed a stronger inhibitory effect on the growth of A549 cells (Figure 2B). The effect of sCS NPs-HA on the proliferation of A549 cells increased with time. The inhibitory effect on A549 cells gradually increased with an increase in the amount of Cy3-labeled siRNA

encapsulated in sCS NPs-HA (0.26, 0.52, or 0.78 μg). Nevertheless, this effect was absent in other test groups. Thus, sCS NPs-HA were demonstrated to have an obvious advantage: inhibition of the proliferation of A549 cells.

Efficiency of transfection of CS NPs into A549 cells

The results of the flow-cytometric analysis (Figure 3) showed that the transfection rate of sCS NPs-HA in A549 cells was higher than that of other NPs at 24 hrs, and the difference was statistically significant, when all experimental groups were incubated with equal amounts of Cy3-labeled siRNA (2.6 μg). By contrast, no significant difference was observed in the transfection efficiency between sCS NPs and Cy3-labeled siRNA. At 48 hrs, the transfection efficiency rates of the three groups all
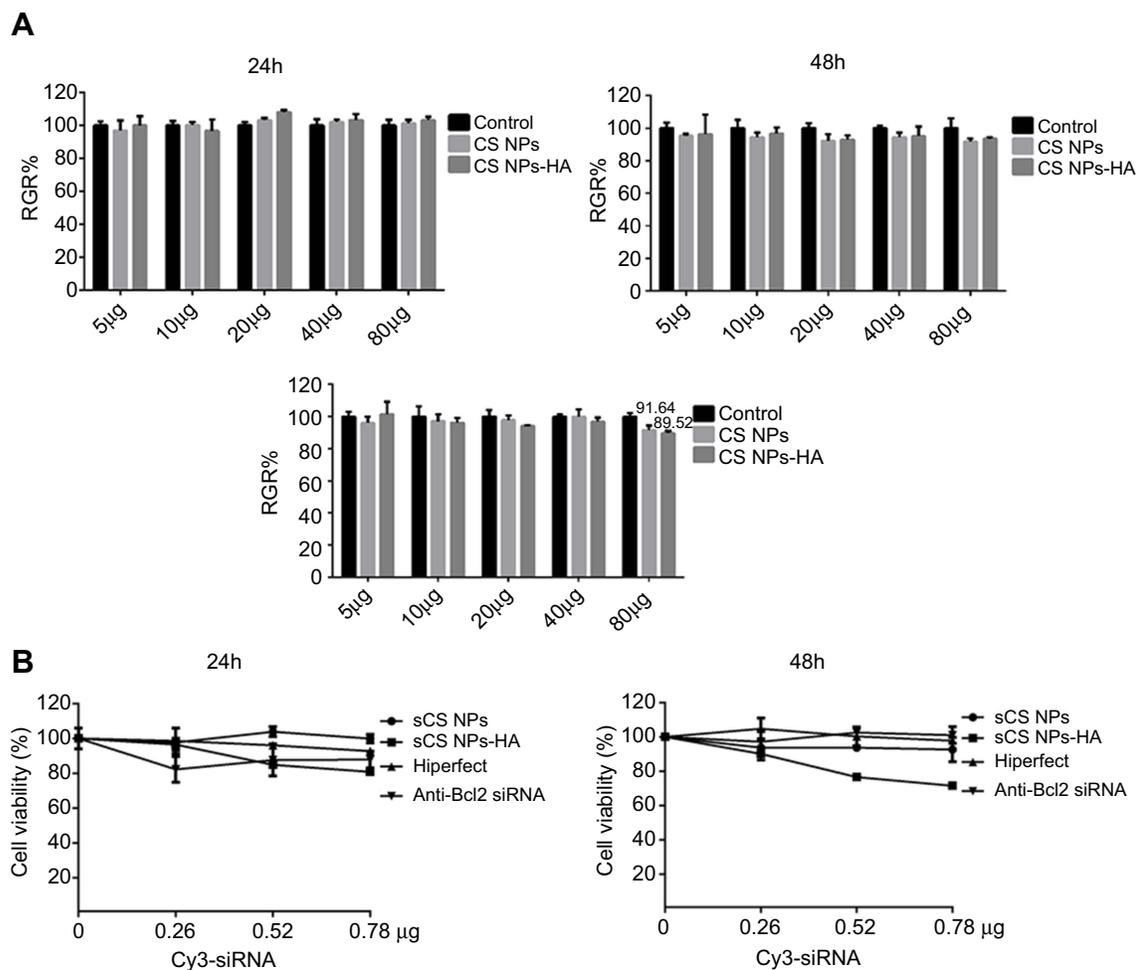

Figure 2 Cytotoxicity and proliferation of A549 cells treated with various NPs. (**A**) Cytotoxicity of CS NPs and CS NPs-HA (5, 10, 20, 40, 80 μg). No significant change was observed in the growth rate of L929 cells treated with different NPs until 96 h (n=3) (Two-way ANOVA). (**B**) Effects of sCS NPs-HA on the proliferation of A549 cells. This assay uncovered an obvious advantage: inhibition of the proliferation of A549 cells (0.26, 0.52, 0.78 μg).
Abbreviations: CS NPs, chitosan nanoparticles; CS NPs-HA, HA-modified chitosan nanoparticles; sCS NPs, chitosan nanoparticles loaded with siRNA; sCS NPsHA, HA-modified chitosan nanoparticles loaded with siRNA; Hiperfect, siRNA transfection; Anti-Bcl2 siRNA, naked siRNA.
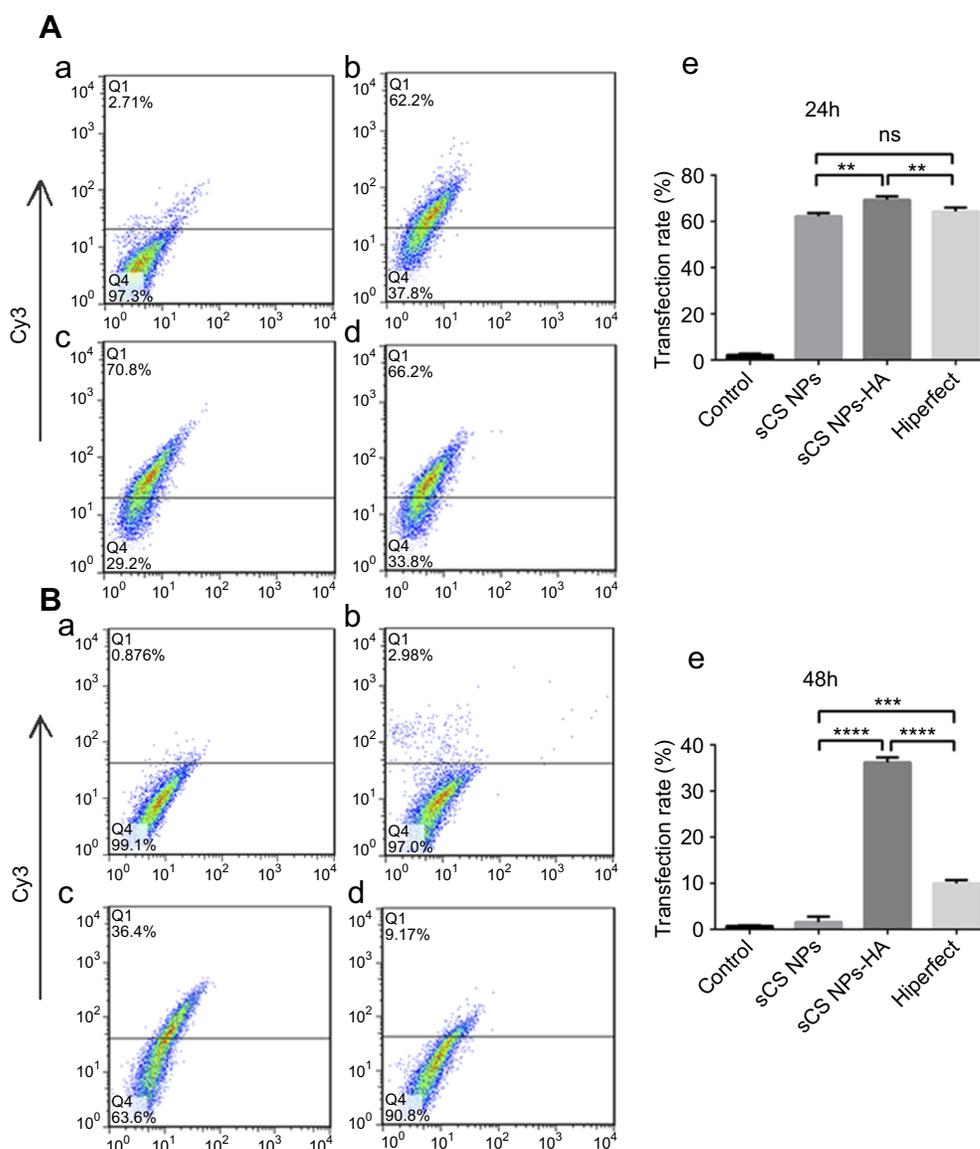
Figure 3 Efficiency of transfection of sCS NPs, sCS NPs-HA, and Cy3-labeled siRNA (Hiperfect transfection) into A549 cells at 24 hrs (**A**) and 48 hrs (**B**) (amounts of Cy3-labeled siRNA 2.6 µg) (n=3). a) Control, b) sCS NPs, c) sCS NPs-HA, and d) Cy3-labeled siRNA, e) statistical analysis of transfection rates. In comparison with the Cy3-labeled siRNA transfection group, the sCS NPs-HA group had higher transfection efficiency and the difference was statistically significant. ***$P<0.001$, ****$P<0.0001$ (one-way ANOVA (and nonparametric) and t-tests), ns means not statistical significance.

decreased, but that of sCS NPs-HA was still the highest, and the differences between sCS NPs-HA and others were statistically significant. Thus, sCS NPs-HA facilitated and prolonged the release of the Cy3-labeled siRNA via high transfection efficiency.

The immunofluorescent assay

To evaluate the effect of sCS NPs-HA binding to their receptor CD44, changes in CD44 expression were examined in the immunofluorescent assay. sCS NPs-HA group transfection Cy3-siRNA amount is 0.52 µg. CD44 stained with green fluorescence, whereas sCS NPs-HA manifested the red

fluorescence of Cy3-siRNA. As depicted in Figure 4, the red fluorescence was mainly distributed in the cytoplasm; in comparison with the control group, the sCS NPs-HA group showed greater green fluorescence, which was mainly dispersed in the cytomembrane, which was the brightest at the edge of A549 cells at 4 hrs. By contrast, fluorescence was strong around the nucleus in the control group. These observations indicate that receptor CD44 maybe activate by HA of sCS NPs-HA, and the amount of sCS NPs-HA entering cells increased with gradual activation of CD44. The results of PCR showed that the expression of CD44 changed with time. The expression of CD44 was more than two times that of the
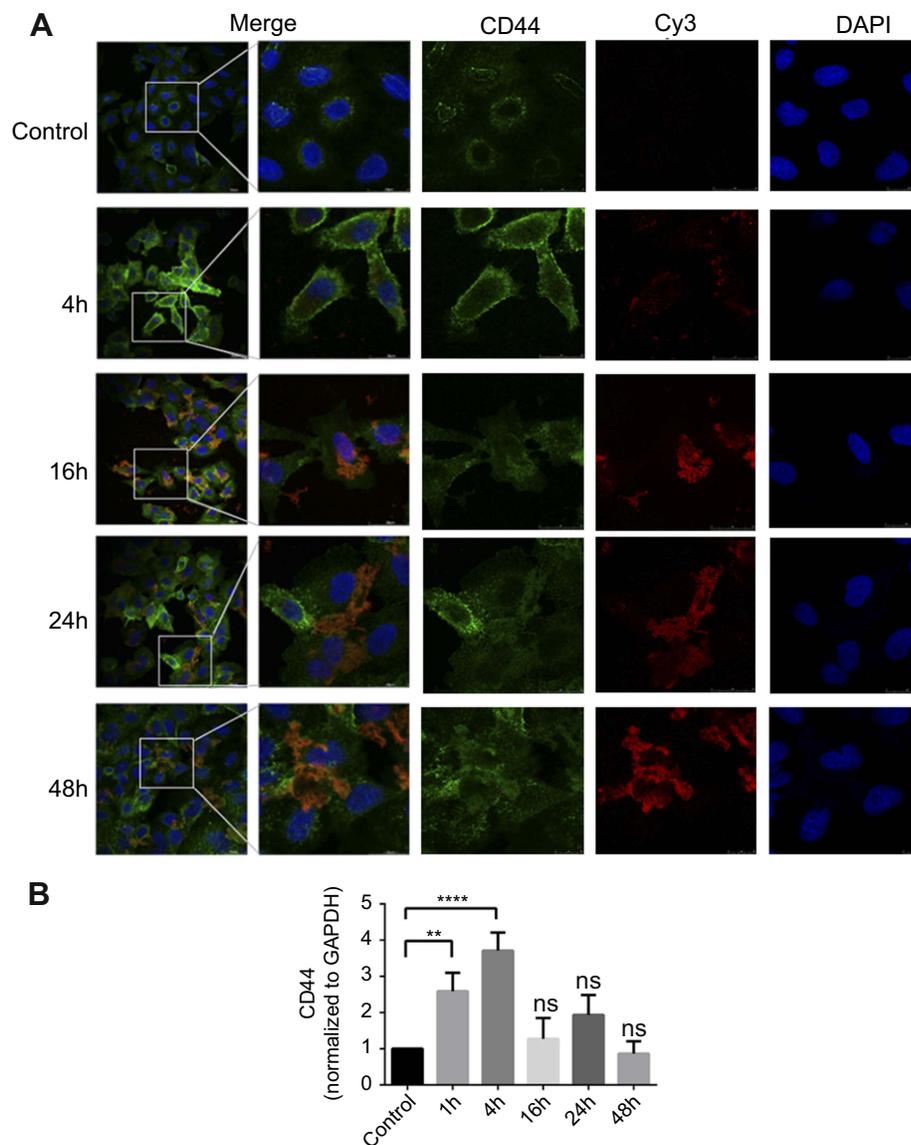
Figure 4 (**A**) Changes in the fluorescence intensity of sCS NPs-HA and receptor CD44 at different time points. Red, green, and blue fluorescence correspond to sCS NPs-HA, CD44, and nucleus, respectively (amounts of Cy3-labeled siRNA 0.52 μg). (**B**) CD44 expression changes over time. **P<0.01, ****P<0.0001 (one-way ANOVA (and nonparametric) and t-tests), ns means not statistical significance.

control group at 1 hr, and the expression of CD44 was more than three times that of the control group at 4 hrs. At 16, 24, and 48 hrs, the expression of CD44 was decreased compared to 1 and 4 hrs (Figure 4B). Thus, the newly prepared sCS NPs-HA maybe could mediate the entry of Cy3-labeled siRNA into A549 cells through the activated receptor: CD44.

Effects of sCS NPs-HA on the target gene

The effects of CS NPs, sCS NPs, CS NPs-HA, sCS NPs-HA, and transfection with Cy3-labeled siRNA on A549 cells were assessed through analysis of the expression of target gene *BCL2* by Western blotting, when all experimental groups were incubated with equal amounts of Cy3-labeled

siRNA (0.52 μg). Figure 5A shows that the expression of the *BCL2* protein in CS NPs, sCS NPs, and CS NPs-HA groups did not decrease compared with the control. The group treated with Cy3-labeled siRNA transfection and sCS NPs-HA showed reduced expression of *BCL2*, and there was no statistical difference between the two groups. These results show that sCS NPs-HA effectively carried the Cy3-labeled siRNA into A549 cells and performed their function and were equivalent to the role of transfection reagents. In addition, the fluorescence intensity was the brightest in the sCS NPs-HA group at 48 hrs, followed by the group treated with the Cy3-labeled siRNA transfection. The fluorescence intensity was the weakest in the group treated with sCS NPs
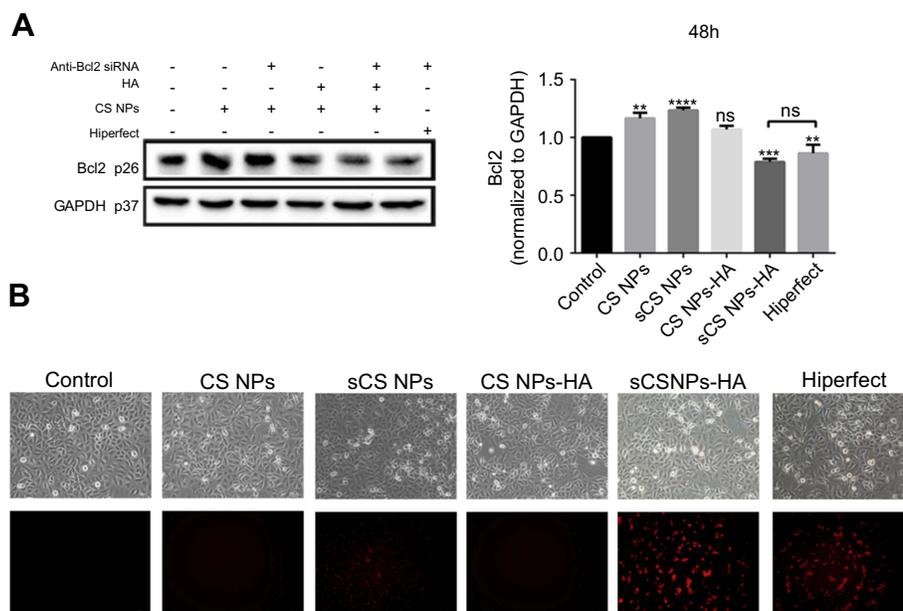
Figure 5 Effects of the Cy3-labeled siRNA loaded by NPs on the target gene (amounts of Cy3-labeled siRNA 0.52 μg). (**A**) Expression of the *BCL2* protein in A549 cells, as determined by Western blotting and normalized to GAPDH expression at 48 hrs. Data are presented as mean ± SD of three experiments. **$P<0.01$, ***$P<0.001$, ****$P<0.0001$ (one-way ANOVA (and nonparametric) and *t*-tests), ns means not statistical significance. (**B**) Fluorescence microscopy images at 48 hrs.

(Figure 5B). These observations indicate the advantages of the prolonged and sustained release of Cy3-labeled siRNA from HA-modified CS NPs. The the stained release properties of HA may support this result, but there is currently no clear experiment to verify.

In vivo gene silencing and tumor-targeting effects
Effects on tumor growth
To investigate the effects of sCS NPs-HA on tumor growth, a tumor xenograft mouse model was established via injection of human A549 cells into the underarms of female BALB/c mice. When tumor volume of a mouse reached 60 ±10 mm³, PBS, sCS NPs, sCS NPs-HA, or naked Cy3-labeled siRNA were injected through the tail vein every other day, the injection dose of Cy3-labeled siRNA in all experimental groups was 0.16 mg siRNA/kg. After 20 days (day 35 post-tumor inoculation), the mice were euthanized, and tumors were removed for Western blotting and frozen sections. As illustrated in Figure 6A, the tumor size in the group treated with sCS NPs-HA was much smaller than that in other groups; similarly, the growth of subcutaneous tumor volume in the sCS NPs-RNA group was significantly inhibited. Compared with the PBS group, the weight of tumors in the sCS NPs-HA group was significantly smaller, and this difference was statistically significant; differences in other groups were not significant. After the mice were euthanized,

weights of their body, liver, kidneys, and spleen were measured. The changes in liver, kidney, or spleen indices in each experimental group were statistically analyzed (Figure 6B). In comparison with the control group, the experimental groups showed no significant difference in the liver, kidney, and spleen indices ($P>0.05$), indicating that the newly prepared CS NPs caused no significant toxicity to murine organs. All these results suggested that sCS NPs-HA prepared in this study inhibited tumor growth without obvious organ toxicity in the mouse model.

In addition, to detect RNA interference with the target gene, Western blotting was carried out to analyze *BCL2* protein expression in tumor tissues. In comparison with the control group, there were no silencing effects in groups naked Cy3-labeled siRNA and sCS NPs. The group treated with sCS NPs-HA manifested obvious silencing of the *BCL2* gene in comparison with the other groups (Figure 6C). In conclusion, sCS NPs-HA maybe could localized at the tumor site suppressed the target gene.

Discussion
Gene therapy has promising therapeutic applications, and the use of siRNA for gene therapy has attracted attention of several researchers.[40] siRNA as an effective gene therapy tool can silence a target gene and has been widely applied to gene therapy of tumors.[41–43] Targeted therapy of tumors necessitates the development of a highly efficient carrier for
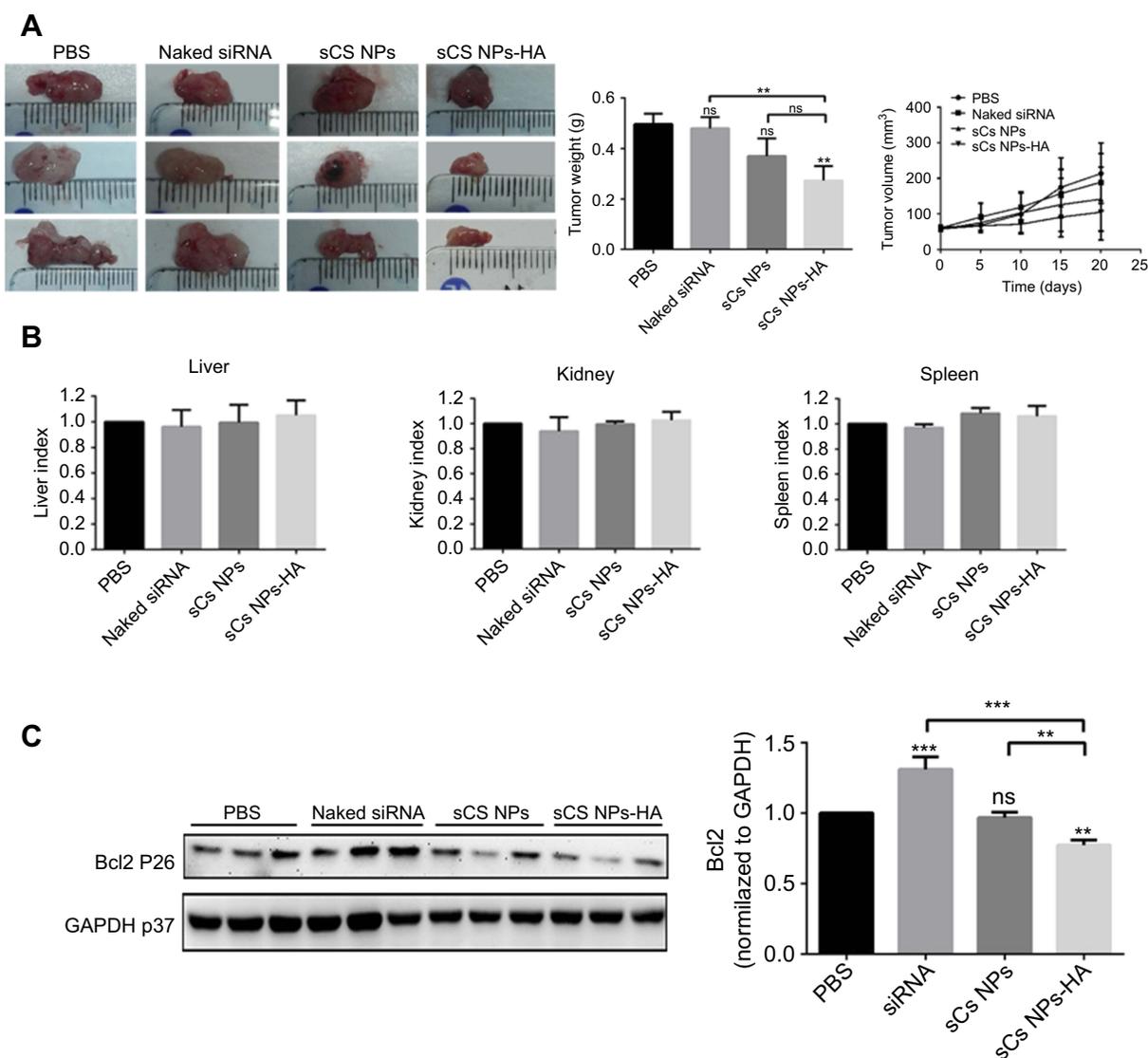
Figure 6 Effects of sCS NPs-HA on tumor growth, the injection dose of Cy3-labeled siRNA in all experimental groups was 0.16 mg siRNA/kg. (**A**) Tumors isolated from murine groups PBS, naked Cy3-labeled siRNA, sCS NPs, and sCS NPs-HA. The weight of tumors in the murine sCS NPs-HA group was significantly lower as compared with the PBS group. **$P<0.01$ (one-way ANOVA (and nonparametric) and t-tests), ns means not statistical significance. The tumor growth inhibition graph showed that the growth of subcutaneous tumor volume in the sCS NPs-RNA group was significantly inhibited. (**B**) The indices (weight ratios) of liver, kidneys, or spleen to the body weight for all groups (n≥3). There were no statistically significant differences between the control and any experimental groups, $P>0.5$ (one-way ANOVA (and nonparametric)). (**C**) Expression levels of the *BCL2* protein in the tumors from mice, as determined by Western blotting and normalized to GAPDH expression. Data are presented as mean ± SD of three experiments. **$P<0.01$, ***$P<0.001$, ****$P<0.0001$ (one-way ANOVA (and nonparametric) and t-tests).

the encapsulation of siRNA. Carriers for siRNA encapsulation include viral and nonviral vectors. Although viral vectors have high efficiency, they are associated with such drawbacks as high immunogenicity and the risk of mutational infection.[44] Nonviral vectors show low transfection efficiency but are relatively safer than viral vectors for gene therapy.[45] Therefore, NP-based polysaccharides such as CS are considered strong candidates for nonviral vectors for gene delivery. The carrier encapsulating siRNA must have high siRNA-loading capacity as well as excellent biocompatibility and low toxicity. CS meets these criteria and is the

only polysaccharide with free amine groups.[46] These functional groups may serve as active sites for various chemical modifications. Smaller CS NPs can prolong their effects in the circulation and evade phagocytosis by macrophages.[47] The size of CS NPs is proportional to the molecular weight of CS.[48] Hence, we chose low-molecular-weight CS as the core material along with TPP for preparation of CS NPs to encapsulate siRNA by ultrasonication.

We prepared CS NPs to encapsulate siRNA and to reduce its degradation in the blood circulation, thereby improving its delivery to a tumor site. The systemic

administration of the siRNA-loaded CS NPs for targeted gene therapy of cancer faces several challenges, including substantial accumulation of the siRNA-loaded CS NPs at off-target sites.[46] Huh et al[49] have reported the development of a tumor-homing glycol chitosan (GC)-based NPs (GS NPs) for the systemic delivery of siRNA. Those authors demonstrated high tumor-targeting and gene-silencing efficiency of GC NPs in vivo. In addition, siRNA delivery carriers are expected to possess a high tumor-targeting ability. Several studies have been conducted on siRNA-loaded CS NPs for the treatment of cancer to improve siRNA targeting to a tumor site. To enhance the tumor-targeting ability of siRNA and to reduce the off-target effects, researchers have coupled CS NP surfaces with targeting moieties specific to tumor cells.[50] An active targeting method exploits overexpression of some ligands or receptors on the surface of tumor cells, and this approach seems more beneficial for the delivery of siRNA to tumor cells. Anna Vanessa et al[23] have taken advantage of the high expression of *MAD2* in NSCLC to develop an EGFR-targeting CS-based system for the delivery of siRNA to selectively silence the *MAD2* mitotic checkpoint gene for the treatment of NSCLC. They demonstrated that this system can downregulate *MAD2* and induce cancer cell death. Shanthi Ganesh et al[51] have encapsulated SSB/PLK1 siRNA in HA-PEI/PEG nanosystems and proved a dose-dependent and target-specific *SSB* gene knockdown in sensitive and resistant A549 cells and solid tumors. On the other hand, there have been no reports about siRNA-loaded CS NPs with HA modification that target NSCLC.

HA is a natural polymer with the ability to target its receptor CD44. In addition, the amine backbone of CS allows for chemical modification. On the basis of these features, we chose HA to chemically modify CS NPs and encapsulate Cy3-labeled siRNA. The sCS NPs-HA were employed to deliver Cy3-labeled siRNA to A549 cells overexpressing CD44. We found that the size of sCS NPs-HA is 100–130 nm. It has been reported that CS NPs with a particle size of ~200 nm can be effectively delivered to tumor tissues via heterogeneous vascularization and the "leakage" effect.[39] In addition, the CS NP carrier for siRNA encapsulation should have high siRNA encapsulation capacity. In our experiments, we carried out UV spectrophotometry and agarose gel electrophoresis to demonstrate that the newly prepared CS NPs-HA possess high efficiency of encapsulation of Cy3-labeled siRNA: up to 94%. Furthermore, we noticed stability of sCS NPs-HA

in vitro and found that sCS NPs-HA can retain their properties for a long time, as evident from the negligible changes in the particle size, zeta potential, and PDI. Thus, sCS NPs-HA showed reasonable stability in vitro.

It is important to investigate transfection efficiency and the cell uptake ability of sCS NPs-HA by means of tumor cells for application to targeted gene therapy. The uptake of sCS NPs-HA into A549 cells was studied by flow cytometry. The results revealed that sCS NPs-HA have a higher transfection ability than do sCS NPs and standardized commercial reagents. The transfection efficiency of sCS NPs-HA was more persistent. Nevertheless, sCS NPs-HA had some shortcomings: the rate of sCS NPs-HA transfection into A549 cells was only 36.4% at 48 hrs, although this value is higher than the values reported for sCS NPs and some transfection reagents. In addition, immunofluorescent assays confirmed that sCS NPs-HA can enter A549 cells through the interaction with CD44 as a receptor. The *Bcl2* gene inhibits cell death by blocking the last common channel of the apoptotic signal delivery system, thereby promoting cell survival and thus becoming an important cell survival gene. In this study, we studied the effect of sCS NPs-HA on *BCL2* expression in A549 cells and demonstrated that the expression of *BCL2* decreased in A549 cells treated with sCS NPs-HA, thereby promoting the death of A549 cells, and this effect was stronger than that observed in other experimental groups and statistically significant as compared to the control. This indicates that sCS NPs-HA were efficiently taken up by cancer cells and the silencing of the cell survival gene *Bcl2* was promoted by the delivery of Cy3-labeled siRNA.

Targeting is important for siRNA-loaded NPs. To evaluate the localization of sCS NPs-HA at the tumor site, we conducted in vivo experiments on a mouse xenograft tumor model. We conducted Western blot experiments to assess the expression of the *BCL2* gene in the tumor tissue of each experimental group and found that the *BCL2* gene was significantly more downregulated in the sCS NPs-HA group than in the other groups. In addition, sCS NPs-HA treatment significantly inhibited tumor growth. In general, the newly prepared sCS NPs-HA exerted tumor-targeting effects and prevented the encapsulated Cy3-labeled siRNA from degradation in the systemic circulation, thereby enabling efficient delivery of Cy3-labeled siRNA to the tumor site. As a consequence, HA-modified CS NPs loaded with Cy3-labeled siRNA inhibited the growth of a tumor effectively. Further research should focus on extending the duration of action of sCS NPs-HA in tumors. In addition, the new supercritical fluid (SCF) technology has attracted the

attention of many researchers because of SCF could assist in the preparation of NPs,[52,53] drug delivery,[54] participate in the preparation of composite scaffolds,[55] and destroy the multidrug resistance gene in tumors through a common delivery system.[56] Further research can use SCF with nanocarriers and siRNA to promote targeted therapy of tumors.

Conclusion

HA-modified CS NPs were successfully prepared in this study and manifested low cytotoxicity and high siRNA encapsulation efficiency. In vitro experiments confirmed that sCS NPs-HA can effectively reduce the expression of a target gene (*BCL2*) in A549 cells. In addition, in vivo experiments confirmed accumulation of sCS NPs-HA at the tumor site, thus inhibiting tumor growth. Therefore, HA-modified CS NPs may serve as a promising gene delivery carrier for targeted gene therapy for cancers.

Acknowledgments

Disclosure

The authors report no conflicts of interest in this work.

References

1. Xiao S, Sun S, Long W, et al. A meta-analytic review of the association between two common SNPs in miRNAs and lung cancer susceptibility. *Onco Targets Ther*. 2018;11:2419–2427. doi:10.2147/OTT.S156505
2. Damstrup L, Poulsen HS. Review of the curative role of radiotherapy in the treatment of non-small cell lung cancer. *Lung Cancer*. 1994;11:153–178.
3. Group NM-AC. Chemotherapy in addition to supportive care improves survival in advanced non-small-cell lung cancer: a systematic review and meta-analysis of individual patient data from 16 randomized controlled trials. *J Clin Oncol*. 2008;26(28):4617–4625. doi:10.1200/JCO.2008.17.7162
4. Janku F, Stewart DJ, Kurzrock R. Targeted therapy in non-small-cell lung cancer – is it becoming a reality? *Nat Rev Clin Oncol*. 2010;7(7):401–414. doi:10.1038/nrclinonc.2010.64
5. Rapp E, Pater JL, Willan A, et al. Chemotherapy can prolong survival in patients with advanced non-small-cell lung cancer-report of a canadian multicenter randomized trial. *Am Soc Clin Oncol*. 1988;6(4):633–641. doi:10.1200/JCO.1988.6.4.633
6. Burdett S, Stewart L, Pignon JP. Chemotherapy in non-small cell lung cancer: an update of an individual patient data-based meta-analysis. *J Thorac Cardiovasc Surg*. 2005;129(5):1205;author reply 1205–1206. doi:10.1016/j.jtcvs.2004.12.032
7. Ellis PA, Smith IE, Hardy JR, et al. Symptom relief with MVP (mitomycin C, vinblastine and cisplatin) chemotherapy in advanced non-small-cell lung cancer. *Br J Cancer*. 1995;71:366–370. doi:10.1038/bjc.1995.74
8. listed Na. Chemotherapy in non-small cell lung cancer: a meta-analysis using updated data on individual patients from 52 randomised clinical trials. *BMJ*. 1995;311:899–909. doi:10.1136/bmj.311.7010.899
9. Sun P, Huang W, Jin M, et al. Chitosan-based nanoparticles for survivin targeted siRNA delivery in breast tumor therapy and preventing its metastasis. *Int J Nanomedicine*. 2016;11:4931–4945. doi:10.2147/IJN.S105427
10. Zhou Y-L, Li Y-M, He W-T. Application of mesenchymal stem cells in the targeted gene therapy for gastric cancer. *Curr Stem Cell Res Ther*. 2016;11:434–439. doi:10.2174/1574888X10666151026113818
11. Jin Y, Zhang LZ, Huang Y, Zhang K-N, Xiong B. MiR-182-5p inhibited proliferation and metastasis of colorectal cancer by targeting MTDH. *Eur Rev Med Pharmacol Sci*. 2018;23:1494–1501.
12. Coiffier B, Lepage E, Briere J, et al. CHOP chemotherapy plus rituximab compared with CHOP alone in elderly patients with diffuse large-B-cell lymphoma. *N Engl J Med*. 2002;346(4):235–242. doi:10.1056/NEJMoa011795
13. Druker BJ, Talpaz M, Resta DJ, et al. Efficacy and safety of a specific inhibitor of the BCR-ABL tyrosine kinase in chronic myeloid leukemia. *N Engl J Med*. 2001;344(14):1031–1037. doi:10.1056/NEJM200104053441401
14. Motzer RJ, Hutson TE, Tomczak P, et al. Sunitinib versus interferon alfa in metastatic renal-cell carcinoma. *N Engl J Med*. 2007;356(2):115–124. doi:10.1056/NEJMoa065044
15. Slamon DJ, Shak S, Fuchs H, et al. Use of chemotherapy plus a monoclonal antibody against HER2 for metastatic breast cancer that overexpresses HER2. *Massachusetts Med Soc*. 2001;344(11):783–792.
16. Demetri GD, von Mehren M, Blanke CD, et al. Efficacy and safety of imatinib mesylate in advanced gastrointestinal stromal tumors. *N Engl J Med*. 2002;347(7):472–480. doi:10.1056/NEJMoa020461
17. Fire A, Xu SQ, Montgomery MK, Kostas SA, Driver SE, Mello C. Potent and specific genetic interference by double-strandedRNA in *Caenorhabditis elegans*. *Nature*. 1998;391(6669):806–811. doi:10.1038/35888
18. Youngren-Ortiz SR, Gandhi NS, España-Serrano L, Chougule MB. Aerosol delivery of siRNA to the lungs. Part 2: nanocarrier-based delivery systems. *Kona*. 2017;34:44–69. doi:10.14356/kona.2017005
19. Majumder P, Bhunia S, Bhattacharyya J, Chaudhuri A. Inhibiting tumor growth by targeting liposomally encapsulated CDC20siRNA to tumor vasculature: therapeutic RNA interference. *J Control Release*. 2014;180:100–108. doi:10.1016/j.jconrel.2014.02.012
20. Majumder P, Bhunia S, Chaudhuri A. A lipid-based cell penetrating nano-assembly for RNAi-mediated anti-angiogenic cancer therapy. *Chem Commun (Camb)*. 2018;54(12):1489–1492. doi:10.1039/c7cc08517f
21. Hojat Borna SI, Iman M, Jamalkandi SA. Therapeutic face of RNAi in vivo challenges. *Expert Opin Biol Ther*. 2014;15(2):1–17. doi:10.1517/14712598.2015.973398
22. Haussecker D. Current issues of RNAi therapeutics delivery and development. *J Control Release*. 2014;195:49–54. doi:10.1016/j.jconrel.2014.07.056
23. Nascimento AV, Singh A, Bousbaa H, Ferreira D, Sarmento B, Amiji MM. Mad2 checkpoint gene silencing using epidermal growth factor receptor-targeted chitosan nanoparticles in non-small cell lung cancer model. *Mol Pharm*. 2014;11(10):3515–3527. doi:10.1021/mp5002894

24. Chung YC, Yeh JY, Tsai CF. Antibacterial characteristics and activity of water-soluble chitosan derivatives prepared by the Maillard reaction. *Molecules*. 2011;16(10):8504–8514. doi:10.3390/molecules16108504

25. Sun P, Huang W, Kang L, et al. siRNA-loaded poly(histidine-arginine)6-modified chitosan nanoparticle with enhanced cell-penetrating and endosomal escape capacities for suppressing breast tumor metastasis. *Int J Nanomedicine*. 2017;12:3221–3234. doi:10.2147/IJN.S129436

26. Liu X, Mo Y, Liu X, et al. Synthesis, characterisation and preliminary investigation of the haemocompatibility of polyethyleneimine-grafted carboxymethyl chitosan for gene delivery. *Mater Sci Eng C Mater Biol Appl*. 2016;62:173–182. doi:10.1016/j.msec.2016.01.050

27. Wang T, Hou J, Su C, Zhao L, Shi Y. Hyaluronic acid-coated chitosan nanoparticles induce ROS-mediated tumor cell apoptosis and enhance antitumor efficiency by targeted drug delivery via CD44. *J Nanobiotechnology*. 2017;15(1):7. doi:10.1186/s12951-017-0305-2

28. Xiao B, Ma P, Viennois E, Merlin D. Urocanic acid-modified chitosan nanoparticles can confer anti-inflammatory effect by delivering CD98 siRNA to macrophages. *Colloids Surf B Biointerfaces*. 2016;143:186–193. doi:10.1016/j.colsurfb.2016.03.035

29. Naor D, Sionov RV, Ish-Shalom D. *CD44: Structure, Function and Association with the Malignant Process. Cancer Research*. Vol. 71; 1997:241–319.

30. Nagano O, Saya H. Mechanism and biological significance of CD44 cleavage. *Cancer Sci*. 2004;95(12):930–935. doi:10.1111/j.1349-7006.2004.tb03179.x

31. Thapa R, W GD. The importance of CD44 as a stem cell biomarker and therapeutic target in cancer. *Stem Cells Int*. 2016;2016:2087204. doi:10.1155/2016/1243659

32. Lau WM, Teng E, Chong HS, et al. CD44v8-10 is a cancer-specific marker for gastric cancer stem cells. *Cancer Res*. 2014;74(9):2630–2641. doi:10.1158/0008-5472.CAN-13-2309

33. Quan YH, Kim B, Park J-H, Choi Y, Choi YH, Kim HK. Highly sensitive and selective anticancer effect by conjugated HA-cisplatin in non-small cell lung cancer overexpressed with CD44. *Exp Lung Res*. 2014;40(10):475–484. doi:10.3109/01902148.2014.905656

34. Cortes-Dericks L, Schmid RA. CD44 and its ligand hyaluronan as potential biomarkers in malignant pleural mesothelioma: evidence and perspectives. *Respir Res*. 2017;18(1):58. doi:10.1186/s12931-017-0546-5

35. Hu B, Ma Y, Yang Y, Zhang L, Han H, Chen J. CD44 promotes cell proliferation in non-small cell lung cancer. *Oncol Lett*. 2018;15(4):5627–5633. doi:10.3892/ol.2018.8051

36. Schenk RL, Strasser A, Dewson G. BCL-2: long and winding path from discovery to therapeutic target. *Biochem Biophys Res Commun*. 2017;482(3):459–469. doi:10.1016/j.bbrc.2016.10.100

37. Tsai M-L, Chen R-H, Bai S-W, Chen W-Y. The storage stability of chitosan/tripolyphosphate nanoparticles in a phosphate buffer. *Carbohydr Polym*. 2011;84(2):756–761. doi:10.1016/j.carbpol.2010.04.040

38. Tsai M, Bai S, Chen R. Cavitation effects versus stretch effects resulted in different size and polydispersity of ionotropic gelation chitosan–sodium tripolyphosphate nanoparticle. *Carbohydr Polym*. 2008;71(3):448–457. doi:10.1016/j.carbpol.2007.06.015

39. Nascimento AV, Gattacceca F, Singh A, et al. Biodistribution and pharmacokinetics of Mad2 siRNA-loaded EGFR-targeted chitosan nanoparticles in cisplatin sensitive and resistant lung cancer models. *Nanomedicine (Lond)*. 2016;11(7):767–781. doi:10.2217/nnm-2016-0233

40. Li Y, Yang J, Xu B, Gao F, Wang W, Liu W. Enhanced therapeutic siRNA to tumor cells by a pH-sensitive agmatine-chitosan bioconjugate. *ACS Appl Mater Interfaces*. 2015;7(15):8114–8124. doi:10.1021/acsami.5b00851

41. Chen Y, Gu H, Zhang DS-Z, Li F, Liu T, Xia W. Highly effective inhibition of lung cancer growth and metastasis by systemic delivery of siRNA via multimodal mesoporous silica-based nanocarrier. *Biomaterials*. 2014;35(38):10058–10069. doi:10.1016/j.biomaterials.2014.09.003

42. Atala A. Re: Mg(II)-catechin nanoparticles delivering siRNA targeting EIF5A2 inhibit bladder cancer cell growth in vitro and in vivo. *J Urol*. 2017;198(2):258–259.

43. Jiang K, Li J, Yin J, et al. Targeted delivery of CXCR4-siRNA by scFv for HER2(+) breast cancer therapy. *Biomaterials*. 2015;59:77–87. doi:10.1016/j.biomaterials.2015.04.030

44. Somia I. Gene therapy – promises, problems and prospects. *Nature*. 1997;389(18):239–242. doi:10.1038/38410

45. Merdan T, Kopeček J, Kissel T. Prospects for cationic polymers in gene and oligonucleotide therapy against cancer. *Adv Drug Deliv Rev*. 2002;54:715–758. doi:10.1016/S0169-409X(02)00046-7

46. Huh MS, Lee EJ, Koo H, et al. Polysaccharide-based nanoparticles for gene delivery. *Top Curr Chem*. 2017;375(2):31. doi:10.1007/s41061-017-0114-y

47. Jadidi-Niaragh F, Atyabi F, Rastegari A, et al. Downregulation of CD73 in 4T1 breast cancer cells through siRNA-loaded chitosan-lactate nanoparticles. *Tumor Biol*. 2016;37(6):8403–8412. doi:10.1007/s13277-015-4732-0

48. Jain A, Thakur K, Sharma G, Kush P, Jain UK. Fabrication, characterization and cytotoxicity studies of ionically cross-linked docetaxel loaded chitosan nanoparticles. *Carbohydr Polym*. 2016;137:65–74. doi:10.1016/j.carbpol.2015.10.012

49. Huh MS, Lee S-Y, Park S, et al. Tumor-homing glycol chitosan/polyethylenimine nanoparticles for the systemic delivery of siRNA in tumor-bearing mice. *J Control Release*. 2010;144(2):134–143. doi:10.1016/j.jconrel.2010.02.023

50. Zhong Y, Meng F, Deng C, Zhong Z. Ligand-directed active tumor-targeting polymeric nanoparticles for cancer chemotherapy. *Biomacromolecules*. 2014;15(6):1955–1969. doi:10.1021/bm5003009

51. Ganesh S, Iyer AK, Morrissey DV, Amiji MM. Hyaluronic acid based self-assembling nanosystems for CD44 target mediated siRNA delivery to solid tumors. *Biomaterials*. 2013;34(13):3489–3502. doi:10.1016/j.biomaterials.2013.01.077

52. Kankala RK, Chen B-Q, Liu C-G, Tang H-X, Wang S-B, Chen A-Z. Solution-enhanced dispersion by supercritical fluids: an ecofriendly nanonization approach for processing biomaterials and pharmaceutical compounds. *Int J Nanomedicine*. 2018;13:4227–4245. doi:10.2147/IJN.S166124

53. Kankala RK, Lin X-F, Song H-F, et al. Supercritical fluid-assisted decoration of nanoparticles on porous microcontainers for codelivery of therapeutics and inhalation therapy of diabetes. *ACS Biomater Sci Eng*. 2018;4(12):4225–4235. doi:10.1021/acsbiomaterials.8b00992

54. Kankala RK, Zhang YS, Wang SB, Lee CH, Chen AZ. Supercritical fluid technology: an emphasis on drug delivery and related biomedical applications. *Adv Healthc Mater*. 2017;6:16.

55. Chen B-Q, Kankala RK, Chen A-Z, et al. Investigation of silk fibroin nanoparticle-decorated poly(l-lactic acid) composite scaffolds for osteoblast growth and differentiation. *Int J Nanomedicine*. 2017;12:1877–1890. doi:10.2147/IJN.S129526

56. Xu PY, Kankala RK, Pan YJ, Yuan H, Wang SB, Chen AZ. Overcoming multidrug resistance through inhalable siRNA nanoparticles-decorated porous microparticles based on supercritical fluid technology. *Int J Nanomedicine*. 2018;13:4685–4698. doi:10.2147/IJN.S169399